

Soluble polyimides with propeller shape triphenyl core for membrane based gas separation

Agniva Dutta, Soumendu Bisoi, Rajdeep Mukherjee, Rimpa Chatterjee, Rajat K. Das, Susanta Banerjee 

Materials Science Centre, Indian Institute of Technology Kharagpur, Kharagpur 721302, India

Correspondence to: S. Banerjee (E-mail: susanta@matssc.iitkgp.ernet.in)

ABSTRACT: This article reports the synthesis and characterization of a series of new aromatic polyimides (PIs) having bulky tert butyl group containing propeller shaped triphenylamine unit in its structure. The PIs were prepared by the reaction of 4,4'-diamino-4''-(2,4,6-tri-tert-butylphenoxy) triphenylamine with different commercially available aromatic dianhydrides through the formation of corresponding poly(amic acid)s and subsequent thermal cycloimidization. The PIs showed high glass transition temperature (T_g up to 270 °C) and thermal stability (T_{d10} up to 475 °C). The PI membranes showed good mechanical properties with tensile strength up to 70 MPa, excellent separation performance [$P(\text{CO}_2) = 100.8$, $P(\text{O}_2) = 40.4$ barrer], and good permselectivity [$P(\text{CO}_2)/P(\text{CH}_4) = 50.9$, $P(\text{O}_2)/P(\text{N}_2) = 7.6$]. The membranes exhibited extremely high solubility selectivity for the CO_2/CH_4 gas pair due to the strong affinity between CO_2 and nitrogen atoms of tertiary amine in triphenylamine. © 2018 Wiley Periodicals, Inc. *J. Appl. Polym. Sci.* **2018**, 135, 46658.

KEYWORDS: membranes; polycondensation; polyimides

Received 18 December 2017; accepted 27 April 2018

DOI: 10.1002/app.46658

INTRODUCTION

Membrane-based gas separation is a potential cost-efficient and energy saver alternative to traditional separation techniques such as cryogenic distillation and absorption.^{1–3} Polymer membrane technology has been successfully used in different industrial applications such as hydrogen recovery from reactor purge gas, oxygen-enrichment of air for medical purposes, preparation of nitrogen enriched air for food packaging, and stripping of carbon dioxide from natural gas.^{4,5} However, for industrial scale separation applications, polymer membrane materials must exhibit high gas permeability in order to minimize the required membrane area, as well as high selectivity for a given gas pair to achieve sufficient separation and purity.⁶ However, the gas permeation properties of polymeric membrane materials suffer an inherent trade-off between permeability and selectivity as defined by Robeson in his upper bound relationships and later theoretically analyzed by Freeman.^{7,8} The Robeson upper-bound relationship has been regarded as an empirical criterion to judge the integral performance of membranes. Thus, the major criteria for development of new polymers for industrial use are the combination of high permeability and good selectivity by surpassing the Robeson upper bound relationship for different gas pair (CO_2/CH_4 and O_2/N_2 etc.).^{9,10} Rational molecular design is an efficient way to improve the gas transport performance of advanced polymer membranes.

Polyimides (PIs), an important class of engineering plastics, have been extensively used as a primary material for gas separation and fuel cell membranes due to the good gas transport properties, excellent thermal stability and mechanical properties, good film forming ability and low dielectric constant along with solvent and chemical resistance.^{11–14} However, most of the aromatic PIs have a high melting or glass transition temperature and poor processability, due to limited solubility in most organic solvents and infusible nature.¹⁵ This is attributed due to their rigid backbones and strong intermolecular interactions, which restricts their applications.

During the last decade, extensive research has been carried out to modify the molecular interaction of PIs to improve their processability without affecting their positive characteristics. Some of the modifications including, incorporation of kinked structure, cardo and bulky pendent groups in polymer backbone have been effectively hindered interchain packing thus improving the solubility.^{12,16,17} Hence, this modification increases the FFV and rigidity of polymer chains which are essential for improving gas selectivity and permeability.

So far, several polymers with rigid three-dimensional propeller-shaped triphenylamine (TPA) have been developed to investigate gas permeability.^{18–22} The rigid kink structure of TPA increases the stiffness of the polymer which leads to increase of interchain distance and helps to improve both permeability and selectivity.²² In 2008, Chang *et al.* prepared gas permeable PI membranes

based on pendant methoxy-substituted TPA moiety and reported a high selectivity for CO₂/CH₄.¹⁹ Another PI with twisted Me₃TPA by Yen *et al.* showed a high CO₂ permeability and CO₂/CH₄ permselectivity.^{18,20} Recently, Bisoi *et al.* synthesized a polyamide containing trityl substituted TPA and reported a high gas permeability with good selectivity.^{23,24} Along with TPA, the tert-butyl group is also well known for increasing gas permeability in several polymers. Calle *et al.* synthesized a series of tert-butyl-substituted PIs and observed more than threefold increase in gas permeability compared to the pristine one.²⁵

Taking into consideration of the above facts, herein we report a series of novel solution-processable PIs. We have incorporated twisted, three-dimensional propeller-shaped rigid TPA in the polymer backbone with pendent tert-butyl groups, combining the unique properties of both the moieties in polymer repeat unit structure. Thermal and mechanical properties were investigated to assess the capabilities of the prepared PI membranes. It is expected that the combination of the bulky diamine and rigid dianhydrides would produce difficult chain packing, giving a combination of very low chain mobility and high fractional free volume (FFV), which should produce membranes able to approach the Robeson upper bound. The separation performances of these PIs were compared with different commercially available and structurally similar polymers using Robeson diagrams.

EXPERIMENTAL

Materials

2,4,6-Tri-tert-butylphenol, palladium on activated carbon (1 wt %), triphenylphosphite, 4,4'-(hexfluoroisopropylidene)bis(benzoic acid), 1-fluoro-4-nitrobenzene, cesium fluoride (CsF) were purchased from Sigma-Aldrich. 4,4'-(4,4'-Isopropylidenediphenoxy)bis(phthalic anhydride) (BPADA, St. Louis, USA), 4,4'-oxydiphthalic anhydride, 2,2-bis(3,4-dicarboxyphenyl) hexafluoropropane were purchased from Sigma-Aldrich and recrystallized from acetic anhydride followed by heating at 150 °C for 12 h before use. 1-Methyl-2-pyrrolidone, tetrahydrofuran, dimethyl sulfoxide were purchased from Merck, India. *N,N*-Dimethylformamide (DMF) (Merck, India) was purified using NaOH followed by vacuum distillation from P₂O₅ prior to use. CaCl₂ and anhydrous K₂CO₃ (Merck, India) were dried at 140 °C for 12 h before use. The TPA diamine, 4'-diamino-4''-(2,4,6-tri-tert-butylphenoxy) triphenylamine was synthesized using the previously reported procedure.²⁴

Equipments

The carbon, hydrogen, and nitrogen contents of the compounds were analyzed by the pyrolysis method using Vario EL (Elementary, German) elemental analyzer. ¹H-NMR spectra of the polymers and monomers were recorded using Bruker 600 and 400 MHz instruments (Switzerland). ATR-FTIR spectra of the polymer membranes were recorded by NEXUS Nicolet Impact-410 spectrophotometer. Inherent viscosity (η_{inh}) of the polymers at a concentration of 0.5 g/DL in DMAc was measured using an Ubbelohde Viscometer at 30 °C. Gel permeation chromatography (GPC) was performed with an Agilent GPC instrument using DMF (5 g/L LiBr) as eluent and monodisperse poly(methylmethacrylate) was used as standard. RI detector was used to record the signal. Rigaku, Ultima III X-ray diffractometer was used to record the wide angle X-ray diffractogram (WAXD) of the polymers in the range of 5°–40° (2 θ). The Cu-K α

(0.154 nm) source was used, and the instrument was operated at low-intensity beam 40 kV and 40 mA. Average spacing (d_{sp}) were calculated using Bragg equation from amorphous peak maxima. The glass transition temperature (T_g) of all the polymers was determined from the midpoint of the step transition in the second heating run under the nitrogen atmosphere at a heating rate of 20 °C min⁻¹ using TA Q20 DSC instrument. Thermo-oxidative stability of the polymers was studied using TA Q50 thermo gravimetric analyzer under synthetic air (N₂:O₂ = 80:20) at a heating rate of 10 °C min⁻¹. Mechanical properties of the rectangular polymer membranes, of 25 mm length, 10 mm in width, and thickness around 65–75 μ m were determined using H5KS Tinius Olsen UTM with a strain rate of 5% min⁻¹ at 30 °C. The densities (ρ) values of PI membranes were calculated by Wallace High Precision Densimeter X22B (UK) at 30 °C using isocyanate displacement method. The FFV of the polymers were determined from the following eq. (1):

$$FFV = (V - 1.3V_w)/V \quad (1)$$

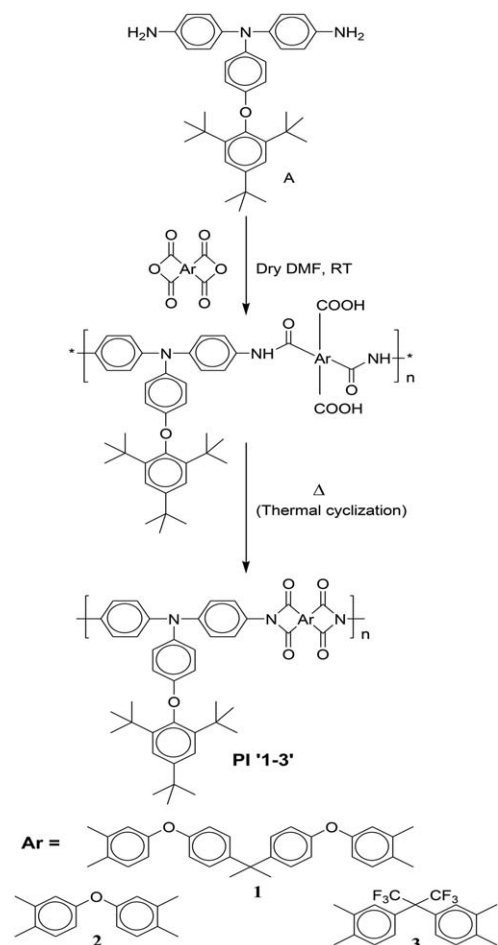
where V is the specific volume ($V = 1/\rho$).

The van der Waals volume (V_w) was measured using the Hyperchem computer program, version 8.0.²⁶ A universal “packing coefficient,” equal to 1.3 is used to convert the van der Waals volume of the repeat units into the “occupied” volume. The dielectric constant (ϵ) of the PI membranes were calculated from the capacitance values from parallel plate capacitor method using a HIOKI 3532–50 LCR Hi Tester at 1 MHz and the temperature of 30 °C in a relative humidity of 45.

The gas permeabilities of four different gasses CO₂, O₂, N₂, CH₄ through the polymer membranes (thickness around 65–75 μ m) were measured using a permeation test system PTS50–16M manufactured by Indian High Vacuum Pumps, Bangalore, India under defined applied gas pressure (e.g., 3.5 bar) at 35 °C. The gas transport properties were measured by the time-lag method in an oven chamber which consists of upstream and downstream parts separated by the membrane. The following eq. (2) was used to calculate the permeability coefficient:

$$P = [VdT_0/Ap_i p_0 T](dp/dt)_s \quad (2)$$

where P is the pure gas permeability expressed in Barrer [$1 \text{ barrer} = 10^{-10} \text{ cm}^3(\text{STP}) \text{ cm cm}^{-2} \text{ s}^{-1} \text{ cm}^{-1} \text{ Hg}^{-1}$], V (cm³) is the downstream volume, d (cm) is the thickness of the membranes, p_i (cmHg) is the difference between the upstream and downstream pressure, T (K) is the measurement temperature, A (cm²) is the effective area of the membrane, T_0 and p_0 are the standard temperature and pressure ($T_0 = 273.15 \text{ K}$, $p_0 = 1.013 \text{ bar}$) and $(dp/dt)_s$ is the rate of pressure rise in the downstream chamber at steady state. The reproducibility of the measurements was checked from four independent measurements using the same membrane (after degassing the membrane for minimum 24 h after each measurement), and it was better than $\pm 5\%$ depending on the nature of gas molecules. For high permeable gases like CO₂ and O₂ the error limit was within 1% to 3% and for low permeable gases like N₂ and CH₄ it was within 2% to 5%. The reported gas permeability values are an average of four independent experiments. The ideal permselectivity ($\alpha_{A/B}$) for separation of A/B was calculated from the ratio of the individual gas permeabilities.



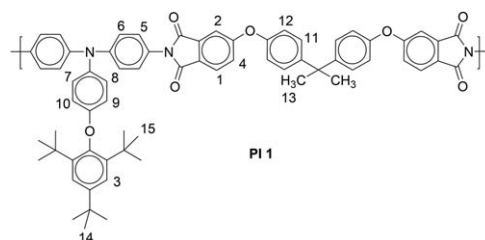
Scheme 1. Reaction scheme of synthesis of the polymers.

$$\alpha_{A/B} = P_A/P_B$$

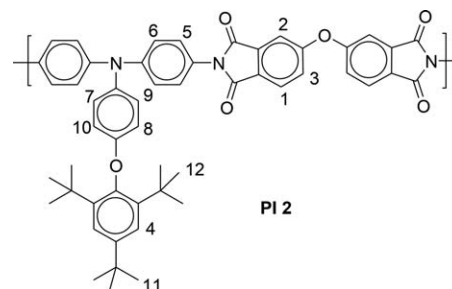
Polymerization and Membrane Preparation

Following the two-step conventional procedure a series of novel PIs were synthesized by reacting, 4'-diamino-4''-(2,4,6-tri-tert-butylphenoxy) triphenylamine (diamine) (A) with three structurally different aromatic dianhydrides in dry DMF (Scheme 1). A representative polymerization procedure is given below.

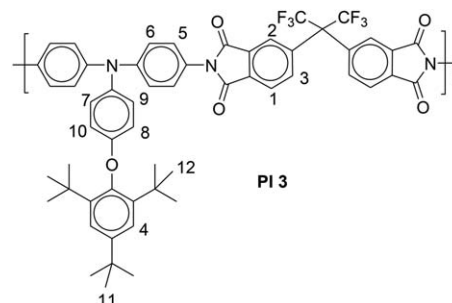
BPADA (0.338 g, 0.65 mmol), diamine (0.377 g, 0.65 mmol), and DMF (7.0 mL) were taken in a 50 mL round bottom flask equipped with a stir bar and CaCl_2 guard tube. The mixture was left for stirring at room temperature, while it transformed into a highly viscous solution of poly(amic acid) (PAA) within 30 min. In the second step, the viscous PAA solution was spread into a clean and dry flat-bottomed Petri dish and kept inside an oven initially at 80 °C overnight for slow removal of the solvent. Finally, the thermal cyclization of the PAA to PI was achieved by sequential heating at 100, 150, 180, 200, 250, and 300 °C, each for 1 h, in an oven under the nitrogen atmosphere. The resulting PI membranes were removed from Petri dish by immersing them in hot water, after that the membranes were dried under vacuum at 140 °C for 24 h. The same procedure was followed for other membranes. The flexible membranes were used for further characterizations.



ANAL. Calcd for $\text{C}_{67}\text{H}_{61}\text{N}_3\text{O}_7$ (1019.45 g mol⁻¹): C, 78.88%; H, 6.03%; N, 4.12%; O, 10.98%. %; found: C, 78.93%; H, 5.85%; N, 4.21%; O, 11.01%. FTIR (cm⁻¹): 2960 (aliphatic C—H stretching), 1783 (C=O asymmetric stretching), 1725 (C=O symmetric stretching), 1600 (aromatic C=C ring stretching band), 1366 (C—O—C asymmetric stretching), 1072, 1006 (C—O—C symmetric stretching), 818 (C—N bending). ¹H-NMR: $\delta_{\text{H}}(\text{ppm})$ (600 MHz, CDCl_3): 7.90 (d, $J = 7.8$, 2H, H1), 7.46 (d, $J = 1.8$, 2H, H2), 7.39 (s, 2H, H3), 7.38–7.31 (m, 5H, H4,5), 7.28 (d, $J = 4.8$, 4H, H6), 7.21 (d, $J = 7.8$, 1H, H7), 7.18 (d, $J = 9$, 4H, H11), 7.12 (m, 1H, H8), 7.06 (d, $J = 8.4$, 4H, H12), 6.96 (d, $J = 8.4$, 1H, H9), 5.97 (d, $J = 7.2$, 1H, H10), 1.79 (s, 6H, H13), 1.37 (s, 9H, H14), 1.32 (s, 18H, H15).



ANAL. Calcd for $\text{C}_{52}\text{H}_{47}\text{N}_3\text{O}_6$ (809.35 g mol⁻¹): C, 77.11%; H, 5.85%; N, 5.19%; O, 11.85%. %; found: C, 77.23%; H, 5.64%; N, 5.22%; O, 11.91%. FTIR (cm⁻¹): 2964 (aliphatic C—H stretching), 1775 (C=O asymmetric stretching), 1720 (C=O symmetric stretching), 1603 (aromatic C=C ring stretching band), 1375 (C—O—C asymmetric stretching), 1080 (C—O—C symmetric stretching), 818 (C—N bending). ¹H-NMR: $\delta_{\text{H}}(\text{ppm})$ (600 MHz, CDCl_3): 8.02 (d, $J = 8.4$, 2H, H1), 7.58 (s, 2H, H2), 7.49 (d, $J = 7.2$, 2H, H3), 7.39 (s, 2H, H4), 7.29 (d, $J = 8.4$, 5H, H5), 7.2 (m, 5H, H6,7), 7.12 (d, $J = 7.2$, 1H, H8), 6.96 (d, $J = 8.4$, 1H, H9), 5.98 (d, $J = 7.2$, 1H, H10), 1.37 (s, 9H, H11), 1.32 (s, 18H, H12).



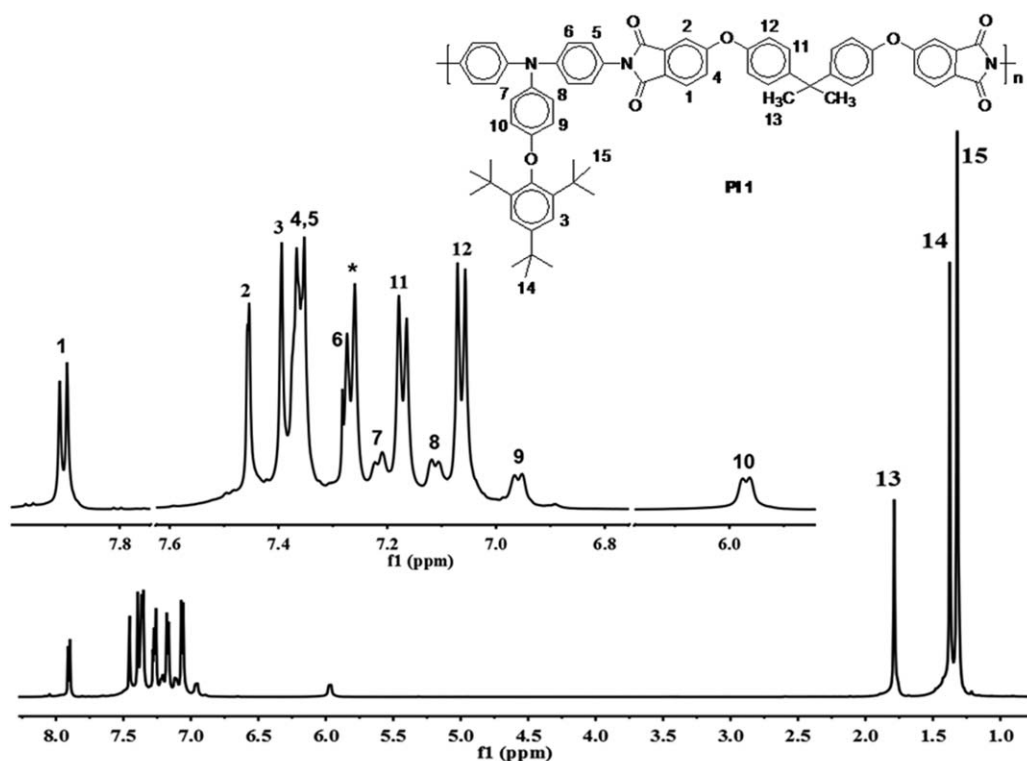


Figure 1. Representative ^1H -NMR spectrum of PI 1 in CDCl_3 (* proton of CHCl_3).

ANAL. Calcd for $\text{C}_{55}\text{H}_{47}\text{N}_3\text{O}_6$ ($943.34 \text{ g mol}^{-1}$): C, 69.98%; H, 5.02%; N, 4.45%; O, 8.47%. %; found: C, 69.78%; H, 5.13%; N, 4.32%; O, 8.85%. FTIR (cm^{-1}): 2960, 2890 (aliphatic C—H stretching), 1780 ($\text{C}=\text{O}$ asymmetric stretching), 1726 ($\text{C}=\text{O}$ symmetric stretching), 1600 (aromatic C=C ring stretching band), 1500, 1430 (C—F stretching), 820 (C—N bending). ^1H -NMR: $\delta_{\text{H}}(\text{ppm})$ (600 MHz, CDCl_3): 8.06 (d, $J = 8.4$, 2H, H1), 7.97 (s, 2H, H2), 7.89 (d, $J = 7.8$, 2H, H3), 7.39 (s, 2H, H4), 7.29 (d, $J = 3.6$, 4H, H5), 7.21 (m, 5H, H6,7), 7.13 (d, $J = 8.4$, 1H, H8), 6.97 (d, $J = 7.2$, 1H, H9), 5.99 (d, $J = 7.8$, 2H, H10), 1.37 (s, 9H, H11), 1.32 (s, 18H, H12).

RESULTS AND DISCUSSION

Polymer Synthesis and Characterization

The PIs were prepared using conventional ring opening polyaddition of three different cyclic dianhydrides with diamine (A) to make poly(amic acid)s intermediate, followed by thermal cyclization (Scheme 1).

The elemental compositions determined experimentally agreed well with the calculated values of the proposed PI structures. The formations of the PIs were also confirmed by ATR-FTIR and ^1H -NMR spectroscopy. The observed characteristic IR absorption bands of imide group near 720, 1775–1783, 1720–1726, and 1370 cm^{-1} were due to C—N stretching, asymmetric, symmetric $\text{C}=\text{O}$ imide ring stretching, and imide ring deformation, respectively, and the absence of characteristic stretching frequencies of poly(amic acid)s near 3200 cm^{-1} (O—H) and 3350 cm^{-1} (N—H) confirms the complete imidization. Figure 1 shows typical ^1H -NMR spectrum of PI 1 in CDCl_3 , all the peaks correspond to an exact number of magnetically different

protons of the repeating unit and also the absence of peak corresponding to amide proton near 10 ppm further supports the complete imidization. Inherent viscosities (η_{inh}), number average molecular weights (M_n), and polydispersity (PDI) values of the PIs (Table I) are in the range of 0.82–0.91 dL/g in DMAc, 93,000–102,000 g/mol and 1.9–2.2, respectively; suggests the higher molecular weight of the polymers.

Polymer Physical Properties

Solubility and Molecular Packing. The solubility of all the PIs was tested quantitatively at 10% (w/v) in various solvents. The PIs were soluble in several common organic solvents like 1-methyl-2-pyrrolidone, dimethyl sulfoxide, DMAc, DMF, DCM, THF, and pyridine. The excellent solubility of PIs was attributed to the insertion of noncoplanar TPA group into the repeat unit

Table I. Physical Properties of the Polyimides

Polymer	η_{inh} (dL/g) ^a	M_n^b (g/mol)	PDI ^c	Density ^d	2θ (°)	d_{sp} (Å) ^e	FFV
PI 1	0.82	93,000	2.1	1.18	17.6	5.0	0.217
PI 2	0.86	97,000	1.9	1.14	18.1	4.8	0.204
PI 3	0.91	102,000	2.2	1.11	15.6	5.6	0.243

^a η_{inh} , inherent viscosity at 30 °C.

^b Number average molecular weight; poly(methylmethacrylate) calibration.

^c Polydispersity index.

^d Density (g/cm^3) measured at 30 °C.

^e d_{sp} , calculated intersegmental distance between polymer chains from Bragg equation.

FFV, The experimentally determined.²⁶

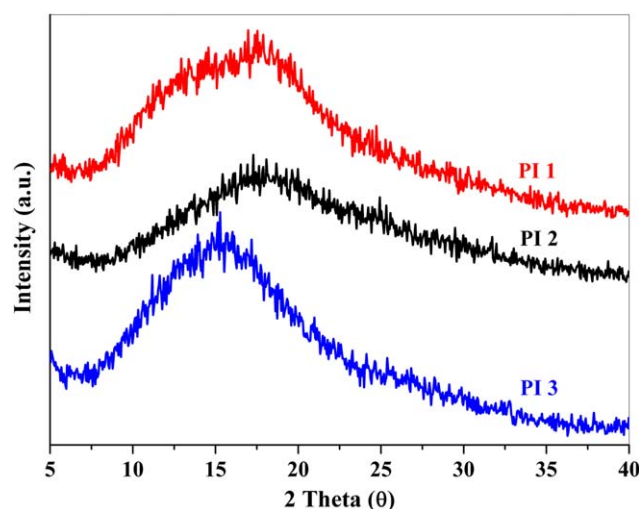


Figure 2. WAXD patterns of the PI membranes. [Color figure can be viewed at wileyonlinelibrary.com]

structure of the PIs and the bulky substituents (i.e., tri-tert-butyl group) that disrupts the polymer chain packing.²⁵

WAXDs are shown in Figure 2, indicating the complete amorphous nature of the polymers.¹⁷ X-ray diffractogram of all PIs show one broad amorphous halo around $2\theta \sim 16^\circ$. The position of the halo maxima of the broad bands of X-rays diffractograms was considered as the inter-segmental distance (d_{sp}) between the PIs chains. The d_{sp} observed decreased in the order: PI 3 (5.6 Å) > PI 1 (5.0 Å) > PI 2 (4.8 Å). The highest d_{sp} of PI 3 in the series is due the presence of $[C(CF_3)_2]$ linkage.¹² The openness of the polymers is measured from the intersegmental distance between the polymer chains, which affects the FFV of the polymers.²⁷ The difference in d_{sp} was also verified by FFV where PI 3 (0.243) > PI 1 (0.217) > PI 2 (0.204). This result is in agreement with WAXD. Hence, with an increase in d_{sp} (Table I) the FFV of the polymers also increased.

Thermal Properties. The DSC curves of the PIs (Figure 3) did not show any crystallization or melting peak, indicating the

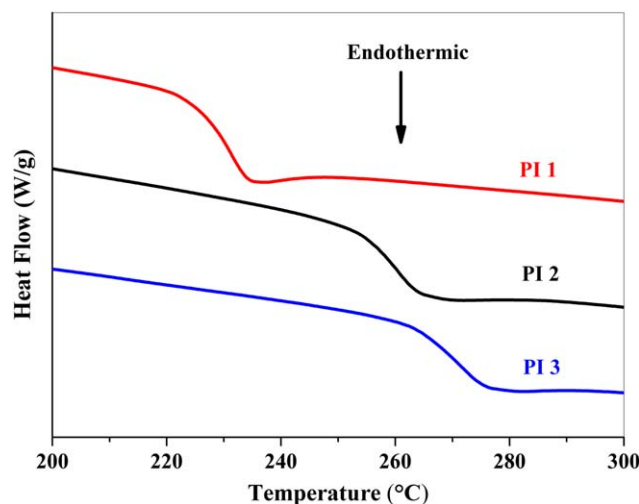


Figure 3. DSC curves of the PIs in second heat scan. [Color figure can be viewed at wileyonlinelibrary.com]

Table II. Mechanical, Thermal, and Electric Properties of the Polyimides

Polymer	TS (MPa)	YM (GPa)	EB (%)	T_g (°C)	$T_{d,10}$ (°C)	ϵ
PI 1	70	1.79	7	230	474	2.90
PI 2	67	2.02	5	260	435	3.10
PI 3	57	2.02	4	270	473	2.50

TS, tensile strength; YM, Young's modulus; EB, elongation at break; T_g , glass transition temperature measured from DSC at heating rate $20^\circ\text{C min}^{-1}$; $T_{d,10}$, 10% weight loss temperature measured from TGA under synthetic air ($N_2:O_2 = 80:20$) at heating rate $10^\circ\text{C min}^{-1}$; ϵ , dielectric constant (ϵ) (1 MHz) and 30°C temperature.

amorphous nature of PIs. The PIs exhibited high glass transition temperature (T_g) values due to the presence of rigid tri-tert-butylphenoxy substituted TPA unit in the polymer backbone, that restricts the segmental motion.²⁰ The T_g values were in the range of 230 – 270°C (Table II) depending on the polymer repeat unit structures. In this series, the PI 1 synthesized from BPADA showed lowest T_g value due to the presence of more number of flexible ether linkages in the dianhydride unit. The highest T_g of the PI 3 was attributed due to the bulky nature of $[C(CF_3)_2]$ linkage.¹²

The TGA thermogram shown in Figure 4 indicated that all the PIs have high thermal stability under synthetic air ($N_2:O_2 = 80:20$) with 10% weight loss temperatures in the range of 420 – 452°C (Table II).

Mechanical Properties. Good mechanical stability is one of the major criteria for membrane based gas separation.²⁸ The mechanical properties of this series are summarized in Table II. The PI membranes had a tensile strength in the range of 57 – 70 MPa with the elongation at break of 4% – 7% and Young's modulus of 1.79 – 2.02 GPa. The PI synthesized from BPADA unit showed comparatively high elongation at break due to the presence of more flexible ether linkages while the 2,2-bis(3,4-dicarboxyphenyl) hexafluoropropane based polymer showed the least elongation at break due to the rigid nature of $[C(CF_3)_2]$ linkage.²⁹

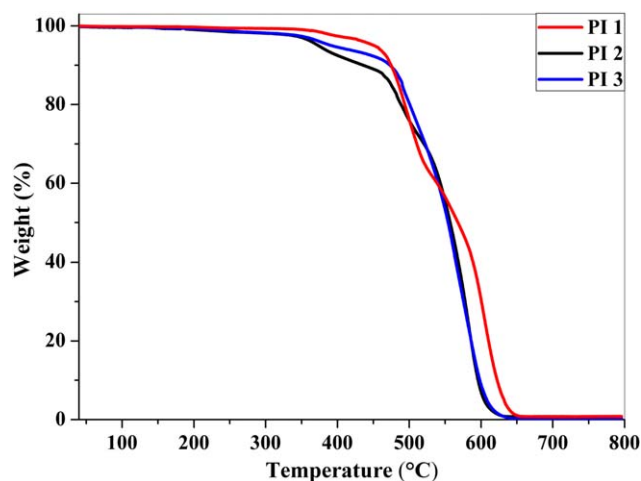


Figure 4. TGA thermograms of the PIs in synthetic air. [Color figure can be viewed at wileyonlinelibrary.com]

Table III. Gas Permeability Coefficient (P) in Barrer and Permselectivities (α) of the Polyimides and their Comparison with Some Other Reported Polymer

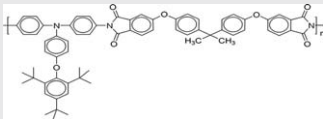
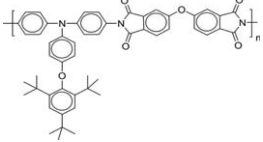
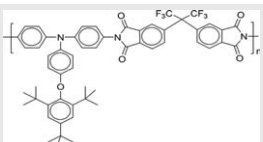
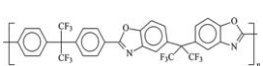
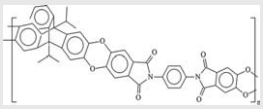
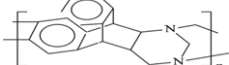
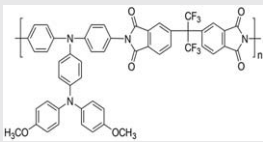
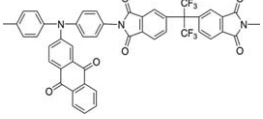
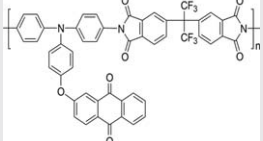
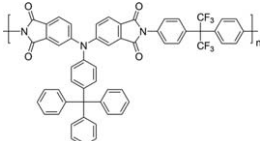
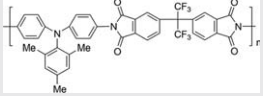
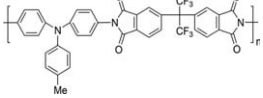
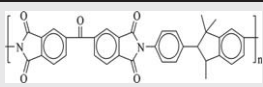
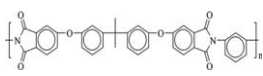
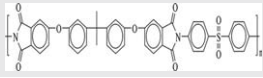
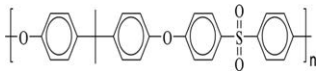
Polymer code	Polymer structure	P (CO ₂)	P (O ₂)	P (N ₂)	P (CH ₄)	α (CO ₂ /CH ₄)	α (O ₂ /N ₂)	Refs.
PI 1		76.2	27.3	3.8	1.58	48.2	7.1	^a
PI 2		64.9	20.5	2.8	1.36	47.5	7.3	^a
PI 3		100.8	40.4	5.2	1.98	50.9	7.6	^a
tTR-450		3575	778	155	80.8	44.2	5.0	¹⁰
KAUST-PI-1		—	542	—	—	—	6.2	³⁰
PIM-TRIP-TB		—	1073	—	—	—	5.7	³⁰
IVb		12.9	2.9	0.59	0.40	32.4	4.9	²⁰
AQ-6FPI		69.9	2.6	2.3	2.43	28.7	1.12	²¹
OAQ-6FPI		57.5	1.5	1.5	1.98	29.0	1.01	²¹
Ia		59.5	14.7	2.9	2.23	26.7	5.0	²²
I-6F		229.2	9.3	7.8	8.9	25.7	1.19	²⁰
II-6F		149.7	5.7	4.8	6.11	24.5	1.19	²⁰

Table III. Continued

Polymer code	Polymer structure	P (CO ₂)	P (O ₂)	P (N ₂)	P (CH ₄)	α (CO ₂ /CH ₄)	α (O ₂ /N ₂)	Refs.
Matrimid		8.7	1.9	0.27	0.24	36.0	7.0	28
Ultem		1.33	0.41	0.05	0.03	36.9	8.0	28
Extrem		3.2	0.81	0.13	0.13	25.2	6.2	28
Polysulfones		5.6	1.2	0.18	0.18	22.0	6.0	24

Gas permeability coefficient (P) in Barrer. 1 Barrer = 10^{-10} cm³ (STP) cm/cm² s cmHg.

^aThis study.

Gas Transport Properties

Effect of Chemical Structure on Gas Transport Properties. The pure gas permeability (P) of the PI membranes for four different gases (CO₂, O₂, N₂, CH₄) were calculated from the steady-state region of the curve, downstream pressure versus time which is measured using the constant volume/variable-pressure method.²⁸ The P and ideal selectivity (α) for the CO₂/CH₄ and O₂/N₂ gas pairs are summarized in Table III.

The P values of the PI membranes follow the trend P (CO₂) > P (O₂) > P (N₂) > P (CH₄). This is in the reverse order of the kinetic diameter (Å) of the gas molecules; CO₂ (3.3) < O₂ (3.46) < N₂ (3.64) < CH₄ (3.8) and also similar like many other aromatic PIs.¹⁷ The P values of these PIs are inversely proportional with the kinetic diameter of the gas molecules. For each gas, the sequence of permeability is was PI 3 > PI 1 > PI 2. The order of gas permeability values of the PIs is in accordance with the FFV values of the polymers and being depended on the dianhydride structure. As compared to traditional PIs (Utem, Extrem, etc.), TPA-PIs exhibited extremely improved gas permeability.²⁸ This can be attributed to the large FFV (0.204–0.243) of these PIs compared to many other reported polymers [FFV_{Utem} = 0.158, FFV_{Extrem} = 0.171].²⁸ Among them, PI 3 showed the highest permeability for CO₂ up to 100 bar. This value surpasses that of commercial PI Matrimid with P (CO₂) around 8.7 bar.³¹ Gas permeability values are highly dependent on FFV following an approximate empirical equation: $P = Ae^{(-B/FFV)}$ where A and B depend on the temperature and type of gas.²⁷ The logarithm of gas permeability values decrease linearly with increase in reciprocal values of FFV, which is a usual trend for all the polymers (Figure 5). These polymers also showed improved gas permeability in comparison with TPA based polyamides (FFV values between 0.089 and 0.188) reported earlier.²⁴ Therefore, high gas permeability of these PIs can be inferred to their high FFV values.

The order of permeability values of the PI membranes for different gases was consistent with the d_{sp} values, as calculated from WAXD, which indicates the order of openness (FFV) between the polymer chains. The PI 3 possesses highest gas permeability value with highest FFV and d_{sp} values in this series due to the presence of bulky [C(CF₃)₂] group. The gas permeability values of PI 1 were greater than PI 2, which is evident

from their FFV and d_{sp} values.²⁴ In the membrane based gas separation technique the permselectivity (α) is more important than permeability (P), as low P can be overcome by decreasing the membrane thickness but low α cannot be improved.³² The permselectivity values varied between 47.5 to 50.9 and 7.1 to 7.6 for CO₂/CH₄ and O₂/N₂ gas pairs, respectively, depending on the polymer repeat unit structures. The high permselectivity of PI 3 is attributed due to the presence of [C(CF₃)₂] group, which not only disrupt the chain packing, but also stiffens of the polymer chain, by restricting the torsional motion of nearby phenyl rings and increase inter-chain interaction due to the polar nature of [C(CF₃)₂] linkage.¹² For O₂/N₂ gas pairs, PI 2 showed high permselectivity compared to PI 1, which is in accordance with their T_g values, with increase in T_g , permselectivity also increases. In the case of PI 1 the presence of extra ether linkage in the polymer repeat unit reduces the stiffness of the polymer backbone (low T_g = 230 °C), which resulted with low selectivity.

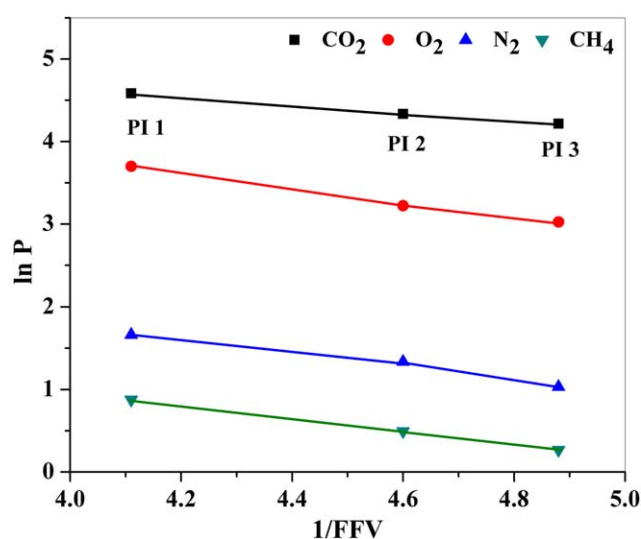


Figure 5. The dependence of gas permeability versus reciprocal of fractional free volume of the PIs for CO₂, O₂, N₂, and CH₄ gases. [Color figure can be viewed at wileyonlinelibrary.com]

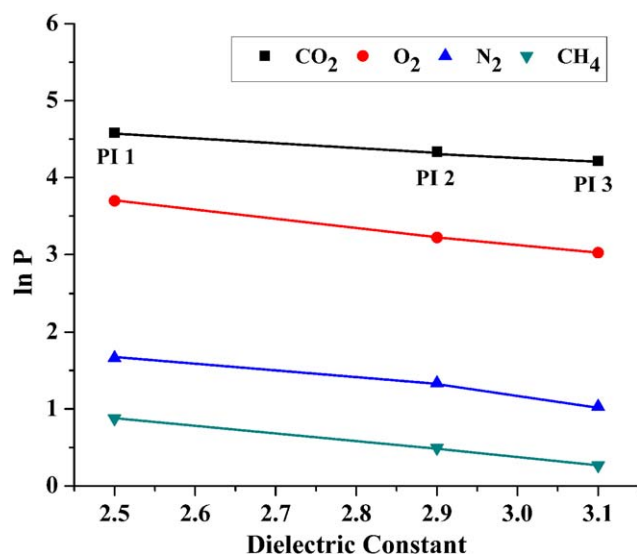


Figure 6. Dependence of gas permeability versus dielectric constant of the PI membranes for CO₂, O₂, N₂, and CH₄ gases. [Color figure can be viewed at [wileyonlinelibrary.com](#)]

According to Matsumoto *et al.*³³ and Miyata *et al.*³⁴ gas permeability is linearly related with the dielectric constant (ϵ), which is a function of the molar polarization and the molar volume of the polymer. So, a higher ϵ signifies higher cohesive force in the polymer, which causes denser chain packing and thus lowers the FFV values. The ϵ values of the PIs are in the range from 2.50 to 3.10 at 1 MHz (Table II) and followed a linear relationship with the gas permeability values (Figure 6). The order of ϵ values was PI 2 > PI 1 > PI 3. PI 3 showed lowest ϵ value in this series due to the presence of [C(CF₃)₂] groups.¹⁵ The low polarizability of C—F bonds and presence of bulky [C(CF₃)₂] group disrupt the polymer chain packing, lowering the ϵ values.¹⁵

Comparison with Other Commercially Available and Previously Reported Polymers. To visualize the influence of the TPA unit in the gas separation efficiency of the PIs, a comparison

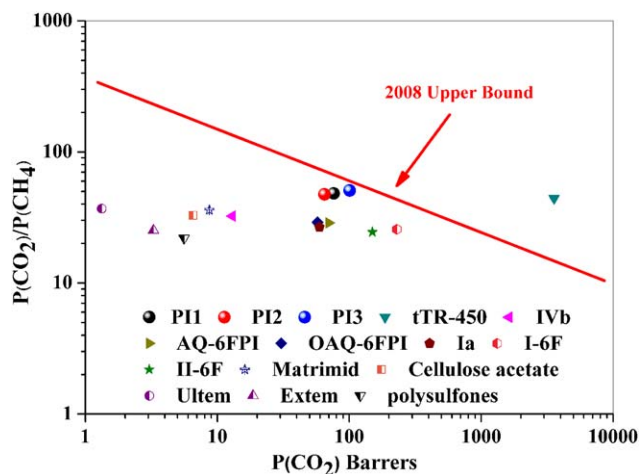


Figure 7. Permeability/selectivity trade-off map for CO₂/CH₄ separation. Values are from this series of PIs and some other reported polymers. [Color figure can be viewed at [wileyonlinelibrary.com](#)]

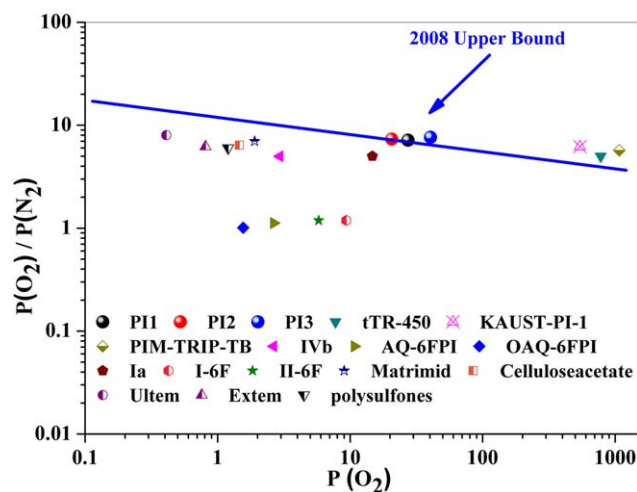


Figure 8. Permeability/selectivity trade-off map for O₂/N₂ separation. Values are from this series of PIs and some other reported polymers. [Color figure can be viewed at [wileyonlinelibrary.com](#)]

has been made with the structurally similar polymers, and other commercially available polymers, such as Matrimid, polysulfones, Ultem and Extem in the form of Robeson plots for CO₂/CH₄, O₂/N₂ gas pairs, shown in Figures 7 and 8, respectively.^{2,8,24} Table III contains all the summarized gas permeation data. Importantly, the data points for TPA-PI membranes are above the Robeson upper bounds for O₂/N₂ gas pairs, in contrast to those of commercially available polymer membranes, which fall below these upper bounds. In particular, two classes of polymers as polymers of intrinsic microporosity and thermally rearranged polymers performs at or beyond the upper bound for different O₂/N₂ and CO₂/CH₄ gas pairs.^{10,17,30} The performance of the present membranes, for the CO₂/CH₄ gas pairs are also encouraging, as other data points also fall below the relevant upper bounds. The membrane performances obtained suggested that PIs containing structures with tri-tert-butylphenol-substituted TPA core are capable of forming large FFV which in turn increases the gas transport properties of the membranes.

CONCLUSIONS

In conclusion, a series of novel bulky aromatic PIs has been designed and synthesized to enable the fabrication of cast membranes suitable for gas permeation studies. The PI membranes demonstrated good solubility in several organic solvents, with high thermal and mechanical stability. In general, the introduction of *t*-butyl substituted TPA unit in the PIs backbone not only helped in achieving high solubility in common organic solvents and easy processibility into membranes, but also increased the gas permeability and the permselectivity. The higher CO₂ permeability resulted from an enhanced solubility coefficient and higher CO₂/CH₄ permselectivity originated from higher solubility selectivity. The superior separation performance accompanied by its good membrane processing ability as compared to most of the conventional PI membranes makes them potential candidates for gas separation applications, particularly those involving CO₂.

ACKNOWLEDGMENTS

The authors are grateful to Debaditya Bera for helping with the synthesis of the diamine monomer. The financial support from the Department of Science and Technology (DST), India (grant no. INT/RUS/RFBR/P-303) is gratefully acknowledged.

REFERENCES

1. Bernardo, P.; Drioli, E.; Golemme, G. *Ind. Eng. Chem. Res.* **2009**, *48*, 4638.
2. Sanders, D. F.; Smith, Z. P.; Guo, R.; Robeson, L. M.; McGrath, J. E.; Paul, D. R.; Freeman, B. D. *Polymer* **2013**, *54*, 4729.
3. Carta, M.; Malpass-Evans, R.; Croad, M.; Rogan, Y.; Jansen, J. C.; Bernardo, P.; Bazzarelli, F.; McKeown, N. B. *Science* **2013**, *339*, 303.
4. Yampolskii, Y. *Macromolecules* **2012**, *45*, 3298.
5. Maier, G. *Angew. Chem. Int. Ed.* **2013**, *52*, 4982.
6. Carta, M.; Croad, M.; Malpass-Evans, R.; Jansen, J. C.; Bernardo, P.; Clarizia, G.; Friess, K.; Lanč, M.; McKeown, N. B. *Adv. Mater.* **2014**, *26*, 3526.
7. Robeson, L. M. *J. Membr. Sci.* **2008**, *320*, 390.
8. Baker, R. W.; Low, B. T. *Macromolecules* **2014**, *47*, 6999.
9. Kim, S.; Jo, H. J.; Lee, Y. M. *J. Membr. Sci.* **2013**, *441*, 1.
10. Robeson, L. M.; Dose, M. E.; Freeman, B. D.; Paul, D. R. *J. Membr. Sci.* **2017**, *525*, 18.
11. Wind, J. D.; Paul, D. R.; Koros, W. J. *J. Membr. Sci.* **2004**, *228*, 227.
12. Ghosh, S.; Banerjee, S. *J. Membr. Sci.* **2016**, *497*, 172.
13. Ganeshkumar, A.; Bera, D.; Mistri, E. A.; Banerjee, S. *Eur. Polym. J.* **2014**, *60*, 235.
14. Hsiao, S. H.; Liou, G. S.; Kung, Y. C.; Chang, Y. M. *J. Polym. Sci. Part A: Polym. Chem.* **2010**, *48*, 2798.
15. Banerjee, S. *Handbook of Specialty Fluorinated Polymers*; Elsevier: Oxford, UK, **2015**.
16. Plaza-Lozano, D.; Comesaña-Gándara, B.; de la Viuda, M.; Seong, J. G.; Palacio, L.; Prádanos, P.; de la Campa, J. G.; Cuadrado, P.; Lee, Y. M.; Hernández, A.; Alvarez, C.; Lozano, A. E. *Mater. Today Commun.* **2015**, *5*, 23.
17. Chatterjee, R.; Ghosh, S.; Bisoi, S.; Banerjee, S. *J. Appl. Polym. Sci.* **2017**, *134*, 45213.
18. Yen, H. J.; Wu, J. H.; Huang, Y. H.; Wang, W. C.; Lee, K. R.; Liou, G. S. *Polym. Chem.* **2014**, *5*, 4219.
19. Chang, C. W.; Yen, H. J.; Huang, K. Y.; Yeh, J. M.; Liou, G. S. *J. Polym. Sci. Part A: Polym. Chem.* **2008**, *46*, 7937.
20. Yen, H.; Guo, S.; Yeh, J.; Liou, G.-S. *J. Polym. Sci. Part A: Polym. Chem.* **2011**, *49*, 3637.
21. Hu, Y. C.; Chen, C. J.; Yen, H. J.; Lin, K. Y.; Yeh, J. M.; Chen, W. C.; Liou, G. S. *J. Mater. Chem.* **2012**, *22*, 20394.
22. Mao, H.; Zhang, S. *J. Mater. Chem. A* **2014**, *2*, 9835.
23. Bisoi, S.; Mandal, A. K.; Padmanabhan, V.; Banerjee, S. *J. Membr. Sci.* **2017**, *522*, 77.
24. Bera, D.; Padmanabhan, V.; Banerjee, S. *Macromolecules* **2015**, *48*, 4541.
25. Calle, M.; García, C.; Lozano, A. E.; Jose, G.; de Abajo, J.; Álvarez, C. *J. Membr. Sci.* **2013**, *434*, 121.
26. HyperChemTM. Professional 7.51; Hypercube, Inc.: Gainesville, FL, **2015**.
27. Bisoi, S.; Bandyopadhyay, P.; Bera, D.; Banerjee, S. *Eur. Polym. J.* **2015**, *66*, 419.
28. Bisoi, S.; Mandal, A. K.; Singh, A.; Banerjee, S. *e-Polymers* **2017**, *17*, 283.
29. Sen, S. K.; Banerjee, S. *J. Membr. Sci.* **2010**, *350*, 53.
30. Swaidan, R.; Ghanem, B.; Pinnau, I. *ACS Macro Lett.* **2015**, *4*, 947.
31. Wang, Z.; Wang, D.; Zhang, F.; Jin, J. *ACS Macro Lett.* **2014**, *3*, 597.
32. Mason, C. R.; Maynard-Atem, L.; Al-Harbi, N. M.; Budd, P. M.; Bernardo, P.; Bazzarelli, F.; Clarizia, G.; Jansen, J. C. *Macromolecules* **2011**, *44*, 6471.
33. Matsumoto, K.; Xu, P.; Nishikimi, T. *J. Membr. Sci.* **1993**, *81*, 15.
34. Miyata, S.; Sato, S.; Nagai, K.; Nakagawa, T.; Kudo, K. *J. Appl. Polym. Sci.* **2008**, *107*, 3933.